ISSN: 2716-9227 Algerian Journal of Engineering and Technology 06 (2022) 009–013 e-ISSN: 2716-9278

Algerian Journal of Engineering and Technology

Journal homepage: https://jetjournal.org/index.php/ajet

Original Article

Study and Evaluation of Electronic transport property for an InAlN based on Monte Carlo

Zakarya Kourdi[a]* and Mohammed Khaouani[b]

[a] *Department ground application system in center of exploitation satellites telecommunication (C.E.S.T), Alger, Algeria.*

[b]*Department of Electricals and Electronics Engineering, Faculty of Technology, University Abou Bekr Balkaid-Tlemcen, Post Box 230, Pole Chetouane, 13000 Tlemcen, Algeria.*

ARTICLE INFO

Article history:
Received 04 December 2021
Revised 29 December 2021
Accepted 28 January 2022

Keywords:
Mocasim;
Tcad-Silvaco;
Monte Carlo;
InAlN/GaN;

ABSTRACT

The emergence of the semiconductors III-N with heterojunction structures has made it possible to study a wide range of two-dimensional phenomena. This paper devotes to simulate the characteristics of the InAlN material, taking into ac-count temperature and doping as dependencies of conduction properties and performance using MOCASIM of the Tcad-Silvaco software. For the electronic transport model analyzing, we adopted most of the predominant mechanisms using various scattering effects including: optical phonon scattering, acoustic phonon scattering through deformation potential and piezoelectric potential, ionized impurity scattering, and grain boundary scattering. As expected, the carrier transports in the GaN layer are affected by the spontaneous polarization of the InAlN layer. To interact that, the diffusion of grain boundaries has been switched from the diffusion of ionized impurities by the deposition of InAlN. In order to achieve the most improvement possible for the electron transferring in terms of thickness and alloy composition related to the improvement of super-deposited layers. The confinement of sub-bands in channel quantum well is also taken into account in the computation of electron mobility. In the end, the adopted electron model is improved by including the effects of deep electron traps.

1. Introduction

Many new transistors based on heterostructures are composed of thin-layer ternary alloys materials epitaxial deposited on a binary substrate. Their operation is based on the existence of heterojunction semiconductor/semi-conductor wide gap or binary semiconductor III-V, as aluminium nitride (AlN), gallium nitride (GaN), indium nitride (InN) and their ternary and quaternary alloys have very attractive properties for microwave applications [1]. Thanks to advances in epitaxial techniques, have been included in the fabrication of active components [2]. The characteristic ability of these structures results to control the flow and distribution of electrons and holes across the shifts bands [3, 4]. The transport phenomena in semiconductor lead to the behaviour of electrons and the energy gap in the conduction band. An analytical study of the problem requires the knowledge of the function of electron energy distri-bution, which is obtained by solving Boltzmann's equation [5]. The latter, partial derivative admits analytical solutions in a limited number of cases. To simulate the electrical transport phenomenon in semiconductors [6, 7], numerical methods are most frequently applied and the Monte Carlo of the written language MocaSim Tcad-Silvaco and the C-Interpreter software as well [8].

This language is not necessarily the best scientific programming, but it is certainly the most widespread and

* *Corresponding author*. Tel.: +213779005472
E-mail address: zkourdi@cds.asal.dz

Peer review under responsibility of University of ElOued.

 DOI: https://doi.org/10.57056/ajet.v6i1.67

under existing programs and programs related to this method.

In this paper, we try to adapt this method to the study of ternary semiconductors [9]. Thus, we precisely apply it to the ternary $In_XAl_{1-X}N$ layer which deposits on GaN layer [10]. We simulate the various interactions, drift velocities transient in all the valleys, and the average drift velocities.

When indium is incorporated into AlN, the variation of the lattice parameter "a" of the compound can be resulted. As a first approximation, this parameter varies linearly with the indium levels. In order to achieve a good lattice matching between InXAl1-XN and GaN, the "x" value must be equal to 0.18, it must incorporate 18% of indium. We then calculate for the alloy $In_{0.18}Al_{0.82}N$ [11]. In addition, for a band gap, it covers a very wide energy range of 0.7 eV (InN) and 6.2 eV (AlN), which gives it a network matching function with 3.4 eV (GaN) [12, 13]. What makes us keep to this choice is the marked resistance to thermal deterioration. This layer is often maintained coherently at hundreds of degrees above the growth temperature until it reaches a temperature of 1100 °C [14], and at least it is recommended to prove the stability of the corresponding grid at no less than 960 °C [15, 16].

In [17, 18, 19], the authors use the program "modelling materials at the atomic scale from first principals initio VASP" in the analysis and approximation of the generalized gradient reported of an InAlN material cubic structure.

Vegard's rule has a linear dependence in composition, with very small deviations that both lattice parameters "a" and "c" essentially exhibit. The research completed as described in the HRXRD and Raman data concluded that even these small deviations of the lattice constant can have an impact on stress computations, so they suggested the following equation for "a" and "c" [20]:

$$\xi(x) = x\xi_{InN} + (1-x)\xi_{AlN} - \delta_{\xi}x(1-x) \; and \; \xi = a, c \qquad (1)$$

Where δ_a = 0.0412 ± 0.0039 Å and δ_c = -0.060 ± 0.010 Å are the corresponding deviation values respectively for the a-cell and c-cell parameters.

2. Results and Discussion

In this paper, the results of research are explained and at the same time the full dis-cussions are given. The results can be presented in the form of figures, graphs, tables and others which allow the reader to understand easily [6, 14]. The discussion can be done in several sub-chapters.

2.1 Non-equivalent interaction intervals

Fig. 1 illustrates all possible transitions of valleys: L-Γ, Γ-X, L-X, X-L, L-X and Γ-Γ (absorption and emission). Interactions between valleys can only occur when the energy carriers are large enough. They are very unlikely to weak field. When an elec-tron is transferred to another valley, the direct effects of interaction itself are added all the discontinuities due to non-equivalence of origin and arrival valleys.

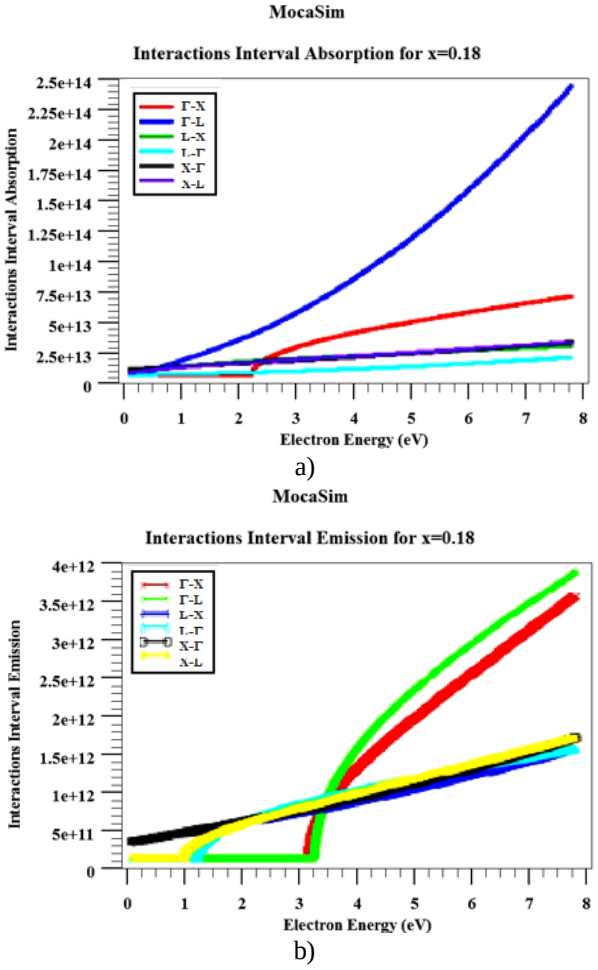

Fig. 1. Non-equivalent interaction intervals of an InAlN material: (a) Interaction intervals absorption and (b) Interaction intervals emission.

In particular, as the kinetic energy of electron is measured from the minimum val-ley which occupies, the transfer to a non-equivalent valley leads to the significant variation of kinetic energy corresponding to the difference in levels between the two valleys [21].

Energy phonons are emitted or absorbed between 8 meV and 42.7 meV, well be-low the initial energy of the carriers at room temperature. As a result, we draw two conclusions: the probability of inter-valley transition Γ-X (removals as emissions) is the most important, and the probability of emissions is greater than removals.

2.2 Scattering Rate

Fig. 2 displays all possible scattering rates for the following valleys: Γ, L and X. One can clearly see that the scattering rate increases with the square root of the energy. The acoustical and optical phonons can also scatter an electron from one valley to another valley. Moreover, the influence of the estimated scattering rate on the total surface simulated the mobility by taking into account the optical pho-non, deformation potential, piezoelectric dislocation scattering and threading with different dislocation densities.

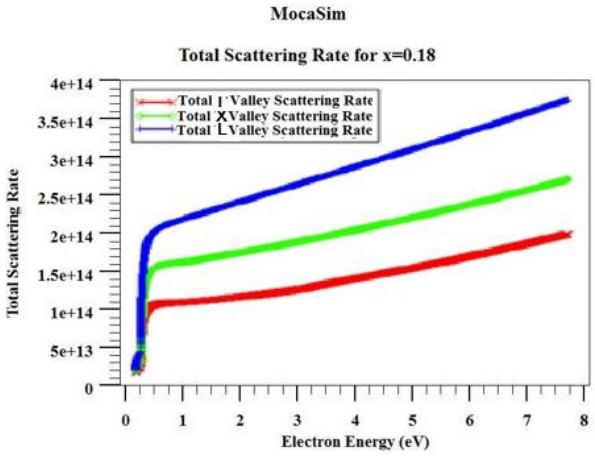

Fig. 2. Inter-valley scattering rate of an InAlN material.

The computation of isotope-induced phonon scattering time is selected by a typi-cal technique for alloy scattering [22, 23] and the Fang Howard wave function [24]. It is inferred that the scattering mechanisms are not necessarily identical, such that many defects add ionized impurity scattering, atomic defects in lattice and long-range scattering in ternary materials.

Generally tend to use the GaN layer NID at n-type doping, this layer has weak n-type conductivity, representing the presence of unintended background donors [25].

Transports widening the heterojunctions between two n-type layers have the same density of impurities, generally the widening of the level is more than large, which makes it difficult to distinguish the impact of each mechanism.

2.3 Effect of temperature on the interaction of mobility and velocity for InAlN

The over-speeding phenomena at high electric fields are due to the smaller relaxation time of the impulse compared to the relaxation time of the energy. In the simulation, cold electrons are injected into the material and accelerated very quickly by the high electric field. Then, the scattering rates increase with energy to suppress the over-speed. The increased scattering rates take some time before it has an effect on the drift velocity. The time delay creates the over-speed effect.

Commonly, the over-speeding variation versus temperature results to the increased temperature gaining electrons of kinetic energy as they rise and collide with other atoms in their energy transfer.

Speed keeps almost the same pace. One can clearly notice that the higher speeds of electron are achieved with a low temperatures, and vice-versa as shown in Fig. 3. As example, when the temperature is equal to a low value 200 K, the electron speed is worth to 2*10-7 cm/s.

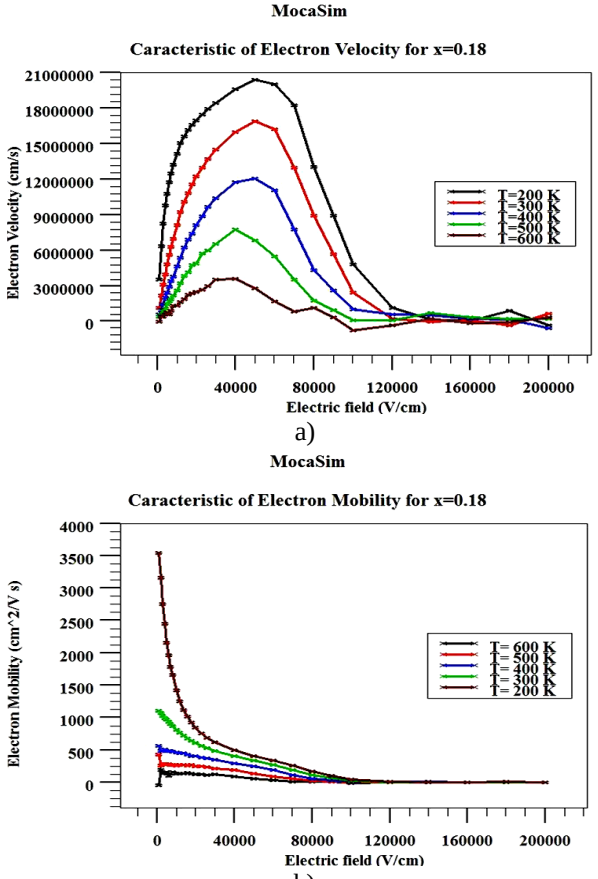

Fig. 3. Mobility and velocity of electrons in the InAlN material relative to the electric field at different temperature values: (a) Electron velocity and (b) Electron mobility.

As temperatures rise, the increased effect of thermal agitation suffered by the at-oms results in a greater possibility of impacts between them. This will lead reducing the free electron rate to 0.25 cm²/Vs as shown in Fig. 3.

2.4 Effect of doping on the interaction of mobility and velocity for InAlN

The variation of velocity for different values doping is taking the same form for all the selected concentrations

(for this reason, we limited to the range concentrations only).

According to Fig. 4, one can clearly observe that the velocity values generally decrease as the concentration increases relative to the electric field. Therefore, the increase in doping can lead to increase the probability of collision between electrons, and this reduces the speed of the electrons. One can also notices, a decrease in peak speed and a minor increase of threshold field.

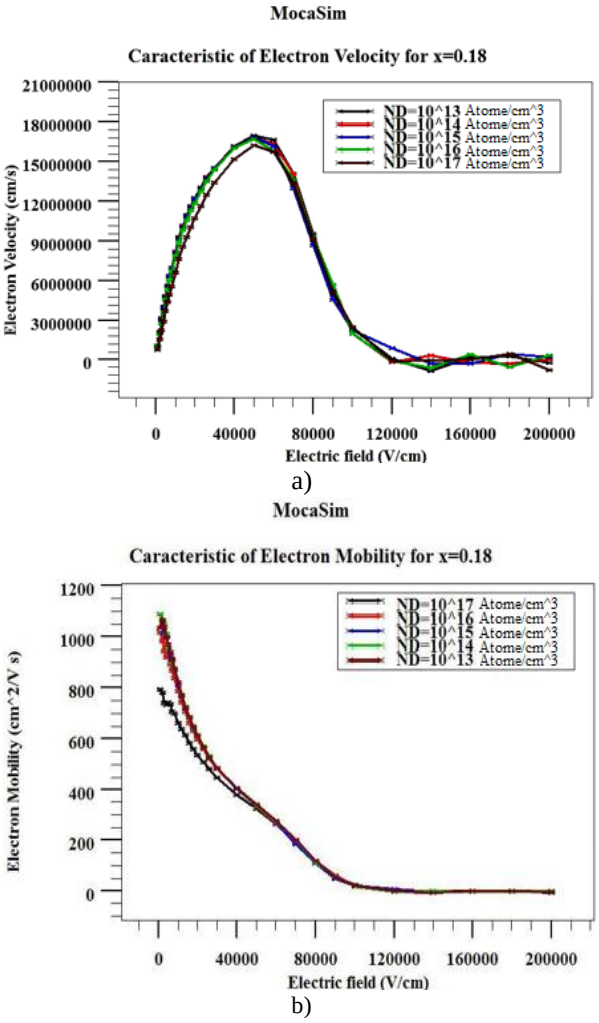

Fig. 4. Mobility and velocity of electrons in the InAlN material relative to the electric field at different doping percentages: (a) Electron velocity and (b) Electron mobility.

Doping has significant effects on weak fields, but the curves tend to merge when-ever the field is very strong. Indeed, when the electric field reaches very high values, the carriers are heated and have less influence on the ionized centres.

Regarding to the saturation velocity, it only appears when doping is weak, which reflects the low dependence of collision mechanisms with large networks on doping, as shown in Fig. 4.

3. Conclusion

This paper has presented the simulations for various interactions and electrical transport in the ternary material $In_{0.18}Al_{0.82}N$ using the Mocasim Tcad-Silvaco soft-ware. It has been shown that the following points can be achieved: (1) The piezoelec-tric interactions are negligible in valleys Γ, X and L, (2) The acoustic interactions are also negligible in the three previous valleys, (3) The inelastic interactions of emission (intervals intra-valleys and optical polar) are more important than those removals, (4) In central valley, the peak over-speed appearing from the critical electric field, they are larger and occur more rapidly when the level of the electric field increases, (5) In the L and X valleys, the speed is lower than in the Γ valley and it can reach the sta-tionary state at about 2 ps. Finally, the transport characteristic can be applied in the nanostructure and electric power, such as: HEMTs heterojunction technology.

Acknowledgements

The authors acknowledge the support of Algerian Space Agency for this work.

References

1. Palacios T, Mishra UK, and Sujan GK. GaN-Based Transistors for High-Frequency Applications, In book: Reference Module in Materials Science and Materials Engineering., 2016.
2. Asahi H, and Horikoshi Y. Molecular Beam Epitaxy: Materials and Applications for Elec-tronics and Optoelectronics, Wiley Optical and Non-Linear Optical Materials., 2019.
3. Schumacher B, Bach H, Spitzer P, and Obrzut J. Electrical Properties', Springer *Hand-book of Materials Measurement Methods*, 2006: 431-484
4. Khuznetsova S, and Kukushkin A. Control Coefficient Application to the Study of Elec-tron Flow Distribution between Linear and Cyclic Electron Transport and the Conditions Es-sential for Appearance of Photosynthetic Oscillations, *Photosynthesis: Mechanisms and Ef-fects*., 1998: 2071-2074

5. Pareschi L, and Russo G. An introduction to Monte Carlo method for the Boltzmann equa-tion, EDB science, 2001.
6. Negol A, Guyot A, and Zimmermann J. A dedicated system for changed particles simula-tion using the Monte Carlo, *Proceeding of IEEE International Conference on systems imple-mentation specific, architectures and processors (AASAP 97).*, 1997.
7. Zimmermann J. Study by the method of Monte Carlo phenomena of electron transport in silicon N-type stationary and non-stationary regimes. Application simulation submicron components, These, 1980.
8. Pesic I. Part Mocasim Overview, Process Simulation Framework Silvaco TCAD interactive tools., 2013.
9. Gupta MC, Ballato, J. Second edition the Handbook of Photonics books, CRC Press Amazon France, 2016.
10. Zhou L, Smith DJ, McCartney MR, Katzer DS, Storm DF. Observation of vertical honeycomb structure in InAlN/GaN heterostructures due to lateral, *Journal Applied Physics Letters*, 2007: 90
11. Mánuel JM, Morales FM, Lozano JG, González D, García R, Lim T, Kirste L, Aidam R, Ambacher O. Structural and compositional homogeneity of InAlN epitaxial layers nearly lattice-matched to GaN. *Acta Materialia*. 2010 ;58(12):4120-4125.
12. Carlin JF, Zellweger C, Dorsaz J, Nicolay S, Christmann G, Feltin E, Butté R, Grandjean N. Progresses in III-nitride distributed Bragg reflectors and microcavities using AlInN/GaN materials. *physica status solidi (b)*. 2005;242(11):2326-2344.
13. Lorenz K, Franco N, Alves E, Watson IM, Martin RW, O'donnell KP. Anomalous ion channeling in AlInN/GaN bilayers: determination of the strain state. *Physical review letters*. 2006;97(8):085501.
14. Wang K, Martin RW, Nogales E, Edwards PR, O'Donnell KP, Lorenz K, Alves E, Watson IM. Cathodoluminescence of rare earth implanted AlInN. *Applied physics letters*. 2006;89(13):131912.
15. Gadanecz A, Bläsing J, Dadgar A, Hums C, Krost A. Thermal stability of metal organic vapor phase epitaxy grown AlInN. *Applied physics letters*. 2007;90(22):221906.
16. Bellakhdar A, Telia A, Coutaz JL. An analytical model for the current voltage characteristics of GaN-capped AlGaN/GaN and AlInN/GaN HEMTs including thermal and self-heating effects. *International Journal of Electrical and Computer Engineering*. 2020;10(2):1791-1804.
17. Darakchieva V, Xie MY, Tasnadi F, Abrikosov IA, Hultman L, Monemar B, Kamimura J, Kishino K. Lattice parameters, deviations from Vegard's rule, and E 2 phonons in InAlN. *Applied Physics Letters*. 2008;93(26):261908.
18. Malmros A, Chen JT, Hjelmgren H, Lu J, Hultman L, Kordina O, Sveinbjörnsson EÖ, Zirath H, Rorsman N. Enhanced mobility in InAlN/AlN/GaN HEMTs using a GaN interlayer. *IEEE Transactions on Electron Devices*. 2019;66(7):2910-2915
19. Kresse G, Furthmüller J. Efficient iterative schemes for ab initio total-energy calcula-tions using a plane-wave basis set, *Physical Review B*. 1996; 54, (16):11169-11186
20. Clemente AV. Structure of InN and alloy layers (In, Al) N Science of materials, University of Caen, 2012.
21. Kaviraj B, Sahoo D. Retraction: Physics of excitons and their transport in two dimensional transition metal dichalcogenide semiconductors. *RSC Advances*. 2021;11(21):25439-25461
22. Ibragimov, G.B.: ʻFree-Carrier Absorption in Quantum Well Structures for Alloy-Disorder Scattering, *Phys. Stat. Sol. (b)*. 2002; 231, (2):589-594
23. Mazumdar K, Pathak GK, Sharan A, Ghoshal A. Mobility and power dissipation due to total phonon scatterings compared with ballistic transport in AlGaN/GaN superlattice. *In 2015 6th International Conference on Computers and Devices for Communication (CODEC)* 2015 Dec 16 (pp. 1-3). IEEE.
24. Mazumdar K, Ranjan RK, Shankar R, Sharan A, Priyadarshini B, Kundu M, Ghosal A. Analysis of electron transport in AlGaN/GaN superlattice HEMTs for isotopes 14N and 15N. *Superlattices and Microstructures*. 2016;100:983-987.
25. Arteev DS, Sakharov AV, Lundin WV, Zakheim DA, Zavarin EE, Tsatsulnikov AF. Carrier mobility in the channel of AlGaN/(AlN)/GaN and InAlN/(AlN)/GaN heterostructures, limited by different scattering mechanisms: experiment and calculation. InJournal of Physics: Conference Series 2019 Nov 1 (Vol. 1400, No. 7, p. 077009). IOP

Publishing.Recommended Citation

Kourdi Z, Khaouani M . Study and Evaluation of Electronic transport property for an InAlN based on Monte Carlo. *Alger. J. Eng. Technol. 2022*, 6:9-13. https://doi.org/10.57056/ajet.v6i1.67